

Development of an Electronic Instrument for Eddy Current Testing

Amir Zacarias Mesquita^{1*}, Daniel Artur Pinheiro Palma², Alexandre Melo de Oliveira³

¹Gamma Irradiation Laboratory, Nuclear Technology Development Center (CDTN), Brazil,

Email: amir@cdtn.br

²Security Assessment Service, Brazilian Nuclear Energy Commission (Cnen), Brazil,

Email: dapalma@cnen.gov.br;

³Physics Department, Federal Institute of Science and Technology of São Paulo, Brazil,

Email: alexandre.melo@ifsp.edu.br

*Corresponding author

Abstract: This article presents the development of a portable electronic variable frequency instrument for eddy current testing. Variations in the conductivity, permeability, or physical characteristics of non-ferromagnetic and ferromagnetic materials cause the impedance of the probe (or coil) connected to a Wheatstone bridge circuit to change. Impedance change causes bridge unbalance, which is indicated by analog and digital indicators on the front panel. The main applications of the equipment are: detection of cracks and surface faults in conductive materials, evaluation of the depths of detected discontinuities, classification of these materials through the variation of conductivity, and evaluation of the thickness of non-conductive layers on a conductive basis. Eddy current testing instruments are superior to equipment that does not use electromagnetic principles for the applications described above. The reason is due to the accuracy and ease of carrying out the inspection. The device developed in this work also has the advantage of the circuits simplicity, the low cost of the electronic components, and the ease of finding them in the market for eventual maintenance. Some test results performed are presented. The instrument performed well for the intended applications.

Keywords: Eddy Current, Electric Current, Electromagnetic, Coil, Nondestructive Test.

I. INTRODUCTION

Among the non-destructive tests, there are those that use electromagnetic principles, the most used being the eddy current test.

Eddy current non-destructive testing has been used for several years in the metal industry, especially in the manufacture of pipes. The foundations of electromagnetic theory on which this test is based were laid down in the mid-19th century by Faraday, Ampère, Maxwell, and others. Most of the theoretical bases for its use in quality control tests were formulated by Förster, Germany, in the 1930s to 1940s. In addition to theoretical work, Förster also developed a large number of instruments to perform various tests [1].

Using a solenoid as shown in Figure 1 and applying an alternating current to it, the magnetic field due to the current varies at the same rate. Approaching a metal plate perpendicular to the coil axis, there will be the formation of induced currents in that part. These currents flow in

concentric closed paths, giving the appearance of an eddy, being perpendicular to the magnetic field.

These are the eddy currents that flow in closed concentric paths perpendicular to the magnetic field. It is important to remember this relationship between electric current and magnetic field, as it helps to decide which type of coil (geometry, dimensions, etc.) is needed to detect faults in a given orientation [2].

Eddy currents induced in the conductive material placed near the coil will also have a magnetic field associated with them. This field, according to Lenz's law, is exactly opposite to the field that caused the eddy currents to flow. The magnetic field, due to eddy currents, will also induce a current in the coil that will be opposite to the current that was already flowing. So, when a metal plate approaches the coil, the coil will have its current slightly reduced. It is this current variation that is used in eddy current tests. The relationship between current, magnetic field of the coil and the plate is shown in Figure 1.

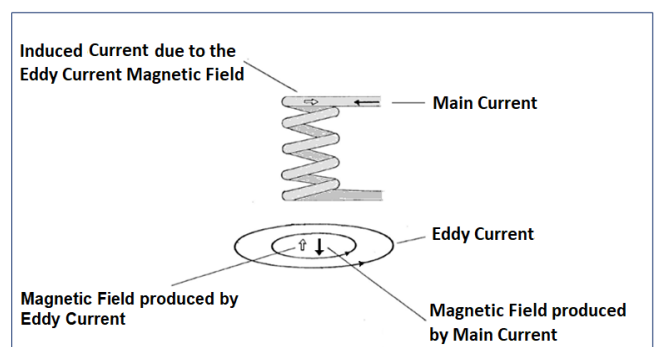


Fig. 1. Relationship between currents and magnetic field of the coil placed next to a metal plate.

Eddy currents are affected by a wide variety of physical and metallurgical conditions in conductive materials. When properly applied, they can be used to investigate various conditions and properties such as: electrical conductivity, heat treatment conditions, structure irregularities, determination of paint layer thickness, measurement of sheet metal thickness and hardness. They can also be used for various types of products, such as sheets, tubes (seamed and seamless), bars, etc. Eddy current inspection is most effective

in locating irregularities near the surface.

This impedance change causes them to be unbalanced, which is indicated by the meters on the front panel. The main applications of the equipment are: detection of cracks and surface flaws in conductive materials, classification of these materials, thickness measurement of metal sheets (with a limitation of up to 6 mm) and assessment of the thickness of non-conductive layers on a conductive base.

A. The Lift-off Effect

The coil with no conductive material in its vicinity will give some indication on the test instrument. As the coil approaches the conductive material, the indication starts to change and continues to change until the coil touches the material. This change in the indication, with the change in the spacing between the coil and the workpiece, is called the lift-off effect, which could be translated as a distance effect. The lift-off is so intense that small variations in the distance between the coil and the part as it travels through the material during inspection can mask some indication of conditions of interest. For this reason, it is normally necessary to maintain a constant distance between the coil and the object under test. When the object having a complex shape is difficult to compensate for the lift-off effect

Eddy current detection instruments can be provided with means to reduce the signals sensitivity from the variation of the distance between the coil and the sample, with the signals on the display coming only from conditions of interest.

This lift-off effect compensation can be done by varying the frequency over a small range, until finding the position for which the sensitivity to small deviations is minimal. That is, even if there is a small variation in the spacing between the probe and the sample, due to the roughness of the part, for example, the display indication does not change. It can always find a point a certain distance away from the metal, where for some frequency, the impedance of the coil has the same magnitude as when it is on the metal. In these two positions, the current in the coil will also have the same magnitude. This principle can also be used to compensate for lift-off, that is, to make the device insensitive to small variations in spacing, and thus only detect signals from variations in conductivity or other parameters of interest [3].

Lift-off signals can be quite inconvenient in some applications. But they can be quite useful in eddy current instruments, for example, for measuring the thickness of non-conductive paints on metals, anodized coatings on aluminum or magnesium alloys and many non-conductive coatings on a conductive base.

II. METHODOLOGY

There is a wide variety of instrument types that can be used for eddy current testing. The use of each type will depend on the purpose of the test and the desired accuracy. In the elaboration of this project, it was defined that its main functions would be:

- Detect surface discontinuities and assess their depths by comparison.
- Classify paramagnetic and diamagnetic materials, according to their electrical conductivities.

All eddy current instruments have certain basic elements in common: an oscillator, a device for detecting the change in

coil impedance, and another for displaying the resulting information. Some instruments include means for analyzing impedance change, others allow signal processing to eliminate certain types of responses, and others provide means for compensating for lift-off signals. The basic block diagram of the eddy current instruments is shown in Figure 2. Below, the main instrumentation elements and the basic operating principle will be described in brief.

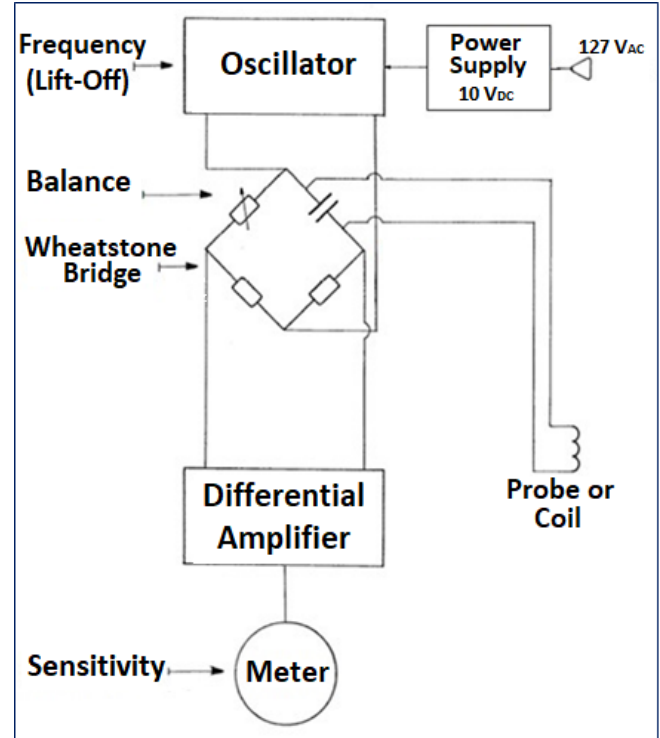


Fig. 2. Block diagram of eddy current instruments.

A. Inspection Coil

The main element of the electrical circuit of the equipment is the inspection coil, whose current produces the magnetic field and induces eddy currents in the metallic material being tested. The coil is designed and built in various ways, depending on how the test will be. The one that will be made for this work will be of the probe type (surface coil). It will be used for testing on sheet metal or other flat surfaces (different types of coil can be made for other applications). The coil, winding and dimensions are calculated using empirical formulas [4,5].

B. Oscillator and Bridge

A variable frequency oscillator produces a signal that is in the kHz range. In eddy current tests, great importance must be given to the choice of frequency, because of the influence of this variable in the tests. The alternating signal is applied to a bridge. A bridge arm is an LC circuit, (tank circuit), where C is a fixed capacitor and L is the inspection coil. When the coil is placed over a part, the bridge can be balanced by an external control. When the coil passes over a discontinuity (crack), the coil impedance will change. The unbalance of the bridge is indicated by changing the position of the pointer of the analog micro ammeter and the digital meter, located on the instrument panel.

1) Oscillator Frequency Range

The main function of the device is to detect and evaluate surface discontinuities (cracks) in non-ferromagnetic materials. Thus, the first parameter to be determined is the frequency band to be used. Low frequencies (about 1 kHz) are used in the inspection of ferromagnetic materials and high frequencies (a few hundred kHz) for non-ferromagnetic materials.

The depth to which the eddy current density is reduced to a level of about 37 % of the surface value is defined as the standard penetration depth. This depth depends on the conductivity and permeability of the material, as well as the frequency of the magnetizing current. For high conductivity, permeability and frequency there will be little penetration.

The depth at which a device can detect a failure can go beyond the standard, depending on its sensitivity and power. It certainly won't go much further, perhaps reaching twice the standard, where the I/I_0 ratio (percentage of surface current intensity) is 13.5 %; or at a point where $I/I_0 = 20$ %. However, to justify the choice of usable frequency range, the standard penetration depth will be taken as a reference.

Equation 1 gives the standard eddy current penetration depth [6].

$$\delta = \frac{1}{\sqrt{\pi f \mu \sigma}} \quad (1)$$

Where:

δ = standard penetration depth in millimeters (mm).

$\pi = 3.1416$

f = excitation frequency in hertz (Hz).

μ = magnetic permeability in henry/mm (H/mm).

σ = electrical conductivity in (% IACS).

It is recommended that the part under test has a thickness of at least three or four times the penetration standard, so that the thickness does not affect the eddy currents.

The IACS - International Annealed Copper Standard is a system that has copper as its electrical conductivity standard. It was established in 1914 by the US Department of Commerce. The electrical conductivity of copper is equivalent to 100 % IACS, which corresponds to 5.8×10^7 S/m (siemens/m), at 20 °C [7,8].

C. Multivibrator

To produce signals in the kHz range, an astable (unstable) multivibrator was used as an oscillator. It provides an approximately square wave whose frequency can be easily controlled. Astable multivibrators are the most commonly used type of relaxation oscillator because not only are they simple, reliable and ease of construction. They also produce a constant square wave output waveform.

Figure 3 illustrates the multivibrator circuit. When the circuit is energized, both transistors start to conduct. If the circuit halves were absolutely identical, T_1 and T_2 would start to conduct together and there would be no multivibrator action. In the real circuit, one of the transistors always starts to conduct first, giving rise to the spontaneous switching process [9,10].

At the two outputs S_1 and S_2 there is a square wave train 180° out of phase. The frequency is determined by the RC constant in the base circuit of the transistor.

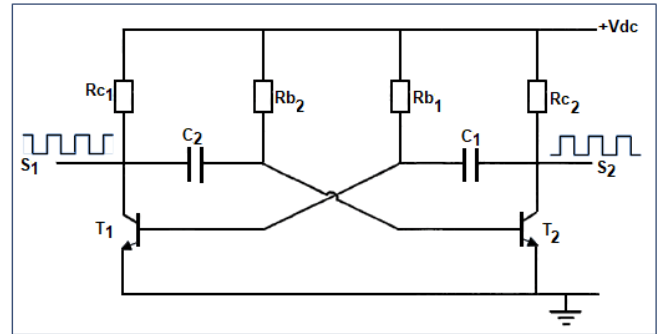


Fig. 3. Astable multivibrator circuit diagram.

D. Frequency Control

The frequency of the multivibrator can be controlled by varying the values of capacitors C_1 and C_2 , or one of the base resistors R_{b1} and R_{b2} according to the equation:

$$f = \frac{1}{RC} \quad (2)$$

In practice, however, large frequency variations (coarse tuning) can only be obtained by changing the values of C_1 and C_2 . Resistors R_{b1} and R_{b2} can only be used for fine tuning. The values of the base resistors in a practical circuit of a self-excited multivibrator are chosen, mainly, to make them efficient producers of polarization conditions and great deviation from the correct polarization value cannot be tolerated [11].

E. Emitter Follower

To separate the multivibrator circuit from the next stage of the circuit, which is the bridge, a common-collector amplifier was used. This amplifier is also known as an emitter-follower, because the output is taken at the emitter and the output signal "follows" the input signal. The main features of this circuit are [12].

- 1 - High input impedance (hundreds of kilohms).
- 2 - Low output impedance (tens of ohms).
- 3 - Voltage gain slightly less than 1.
- 4 - High current gain.
- 5 - Output signal in phase with the input signal.

The combination of high input impedance and low output impedance of this circuit makes it suitable for impedance "matching" between the multivibrator, which has high output impedance, and the bridge, which will have low impedance. In addition, the emitter follower increases the signal strength. Due to these characteristics, it will be used as a separator stage (isolator). Not charging the previous stage and powering the next without showing sensitive load effects.

III. RESULTS

A. Main Instrument Parameters.

1) Frequency

The frequency range chosen was 55 to 220 kHz, with which good results are obtained for most non-ferromagnetic materials and alloys. The following are examples that justify this choice:

- Consider a copper sheet (100 % IACS) whose conductivity is $\delta = 5,81 \times 10^7$ S/m. Using the Equation 1:

$$\delta = 0.14 \text{ mm; for } f = 220 \text{ kHz.}$$

$$\delta = 0.28 \text{ mm; for } f = 55 \text{ kHz.}$$

- Consider an alloy sheet whose conductivity is $\delta = 5.81 \times 10^5$ S/m (1 % IACS). Using the Equation 1:

$$\delta = 1.4 \text{ mm; for } f = 220 \text{ kHz.}$$

$$\delta = 2.8 \text{ mm; for } f = 55 \text{ kHz.}$$

If a frequency well below 55 kHz were used to inspect high conductivity materials, a greater penetration depth would be achieved. But, the ability to detect small discontinuities would be reduced. What is sought, therefore, is an adequate inspection frequency, in which neither the ability to detect very small faults, nor the competence to detect very deep faults, is greatly reduced. It can be seen, therefore, that materials and alloys with conductivity ranging from 1 % to 100 % IACS can be examined for the presence of surface and/or subsurface discontinuities (within a certain limit), using this frequency range.

2) Inspection Coil

The coil built is of the probe type (surface coil). It will be used for testing on sheet metal or other flat surfaces (different types of coils can be made for other applications). The PVC housing shown in Fig. 4 has been machined. The bobbin will be wound into the groove at the end of the stick that is used to handle it. It will induce eddy currents that will flow parallel to the inspected surface. Therefore, transversal to the cracks. The 4.0 mm hole in the stick is for passing the two ends of the coil winding and connecting to the bridge circuit.

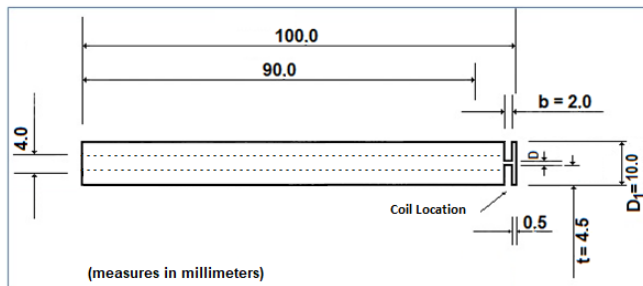


Fig. 4. Diagram of the PVC machined structure to accommodate the inductor coil.

The coil is calculated using empirical formulas. The coil has an air core, the winding is spacing and multi-layered. Using Equation 3, the approximate value of the inductance (L) is found as a function of the coil geometry [13]:

$$L = \frac{2D_1^2 n^2}{25(3D_1 + 9b + 10t)} \quad (3)$$

Where:

L = inductance in microhenrys (μ H).

n = number of turns.

D_1 = actual diameter of the coil in cm, $D_1 = D + 2t$, where D is the internal diameter of the housing (cm).

t = winding height in cm, where: $t = (m - 1/2)d$, where m is the number of layers and d is the wire diameter (cm).

b = length of coil wound (cm).

The wire used was #35 AWG with diameter $d = 0.143$ mm. The winding took up the entire space of the housing groove, which gave about $m = 32$ layers. With the value of $L = 129 \mu$ H using Eq. 3 for the dimensions of Fig. 4, the number of $n = 123$ turns.

After winding the coil, it was taken to an impedance bridge (Type 1650-A from General Radio Company) to check its inductance and the following values were obtained::

$$L = 134 \mu\text{H.}$$

$$R_L = 4.3 \Omega \text{ (direct current).}$$

$$Q = 0.2 \text{ (at a frequency of 1 kHz).}$$

The quality of a coil or Quality Factor (Q) is used to give an indication inductor performance. It is a dimensionless number. The higher the frequency of the alternating current, the higher the inductive reactance. The wire winding has certain resistance components (R). The lower the value of this resistance R , the better the quality of the coil. The Quality Factor (Q) is given by:

$$Q = \frac{2\pi f L}{R} \quad (4)$$

F = frequency in hertz (Hz)

L = inductance of the coil in henry (H).

R = DC resistance component at high frequencies in ohm (Ω).

As the inductance value is a little higher than expected, the resonant frequency was calculated for this new inductance value. Using Equation 5 we have $f_0 = 166.73$ kHz.

$$f_0 = \frac{1}{2\pi\sqrt{LC}} \text{ (Hz)} \quad (5)$$

For a quality factor, $Q > 10$.

3) Signal on the Coil

The voltage across the coil terminals for the various oscillator frequencies was examined with the oscilloscope (Fig. 5). It was observed that despite the excitation not being sinusoidal, a signal with this characteristic was obtained in the probe. With the probe placed in the air, the balance potentiometer cursor was left in its middle position. Acting on the frequency potentiometer of the multivibrator circuit, four frequencies were obtained at which the balance of the bridge occurred. The frequency $f_0 = 166.67$ kHz is the resonant frequency of the tank circuit when the signal is a sinusoid. At other frequencies, the bridge balance also occurs, it is noted that the signal is no longer a perfect sinusoid.

Transistor 2N4410 was used for the multivibrator circuit. It is a switching transistor suitable for use in radiofrequency, of medium power, easy to find on the market and from which it obtained good results in experimental setups [14]. The transistor will work in the saturation region, as its purpose here will be switching [15].

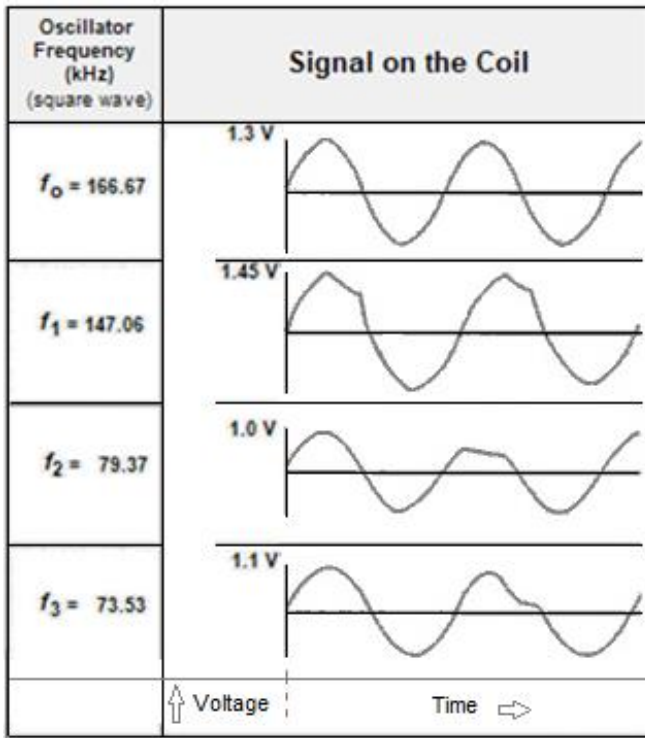


Fig. 5. Waveforms at the tank circuit terminals with the coil in air.

4) Differential Amplifier

As the DC voltage to be measured in the bridge is very small, it was increased using a differential amplifier before being measured. The differential amplifier is a special type of amplifier in which both inputs are floating with respect to ground. The output of an ideal differential amplifier is only proportional to the difference between the signals at each input. The BC557 transistor was used in the differential amplifier circuit.

5) Final Assembly

The complete electronic circuit of the instrument is shown in Figures 6 and 7. The values of all electronic components and their values, in addition to detailed instrument information, can be found in the book of Mesquita (2018) [16].

The signal from the bridge, after passing through the differential amplifier and the emitter follower, will be read by an analog microammeter with full scale of 50 μ A (central zero). It will also be read by a DPM - Digital Panel Meter (scale from -200 mV to 200 mV). The current is on the order of 1 mA, being divided by a shunt resistor in the meter. With microammeter, it is easier to find the operating point of the instrument (lift-off compensation). Because, visualizing the direction of movement of the pointer, it is easier to know the directions of the adjustments of the frequency and balance control potentiometers. With DPM, there is better accuracy and ease of reading the measured values.

With this instrument, only the change in the impedance module is measured. Its operation is simple, presenting only three basic controls to be used:

- Frequency control (lift-off).
- Balance control.
- Sensitivity control.

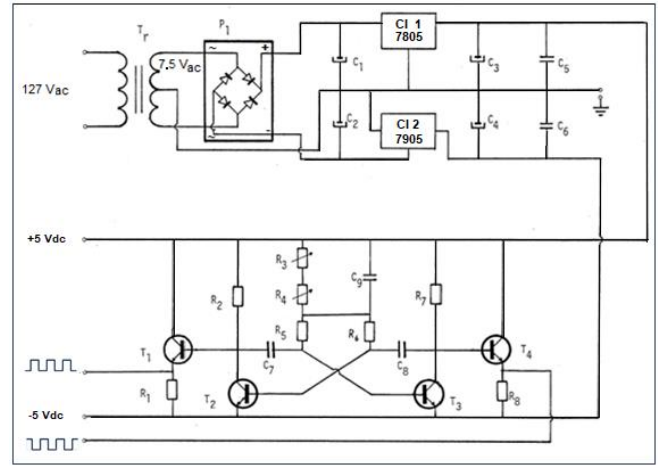


Fig. 6. Source and Multivibrator Electronic Circuit.

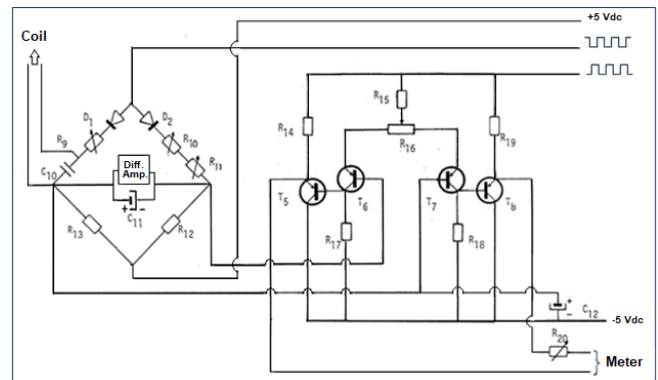


Fig. 7. Bridge, Differential Amplifier and Emitter Follower Circuit.

Figure 8 shows a drawing of the equipment after its assembly.

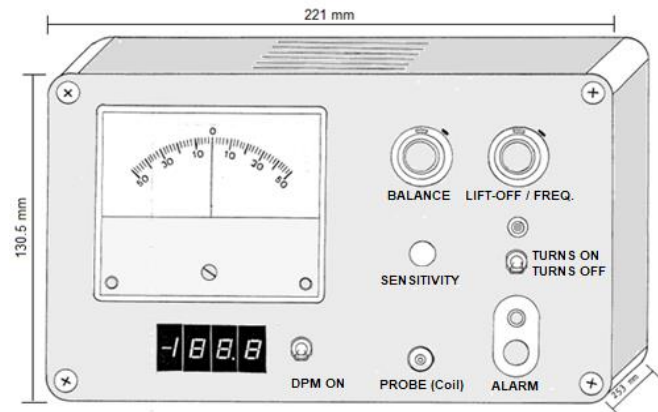


Fig. 8. Front View of Digital Instrument for Eddy Current Tests.

B. Experimental Results

1) Crack Detection

In order to test the instrument for the detection and evaluation of crack depths, some samples of sheets with cracks of various dimensions were machined with an electro-erosion device.

Crack depths were measured using a Leitz-708091 microscope and their surface widths with a Zeiss-29390 microscope.

In all measurements, the controls were adjusted so that the gauges indicated zero, when the probe was in contact with a part of the part without defect. The results presented correspond to the readings of the digital meter (DPM), with the analog meter used only as a reference.

In all tables the readings column does not have engineering units of measurement. They must be converted to the SI System of units of length. For the evaluation of the measurement of cracks, it would be the depth of the crack or its width, keeping one of these dimensions constant. For the evaluation of the insulating layers between the probe and the metallic bases, the thickness of the layer is a function of the alloy or metal and standards must be used. The same procedure must be carried out for the differentiation of metals, that is, known standards must be used. This was not done in this work and will be the subject of other works.

In the graphs below, with the result of each inspection, the curve adjusted by regression is also presented for each test. The value of the coefficient of determination R^2 is also shown.

Some inspections were done in two ways:

A → Corresponds to the results obtained with the instrument compensated for the lift-off effect, varying the frequency.

B → Corresponds to measurements of the same cracks, but without the lift-off compensation. In this case, there is greater sensitivity. It is possible to detect cracks that would not give an indication in A.

a) *INSPECTION No. 1*

Aluminum plate with 9.5 mm thickness. Sensitivity control at minimum.

TABLE I. RESULTS OF INSPECTION No. 1.

Test	Crack Dimensions (mm)		Reading	
	Depth	Width	A	B
0	0.0	0.00	0.0	0.0
1	2.0	0.40	-16.1	-16.1
2	4.0	0.40	-23.5	-23.5
3	6.0	0.40	-26.8	-26.8

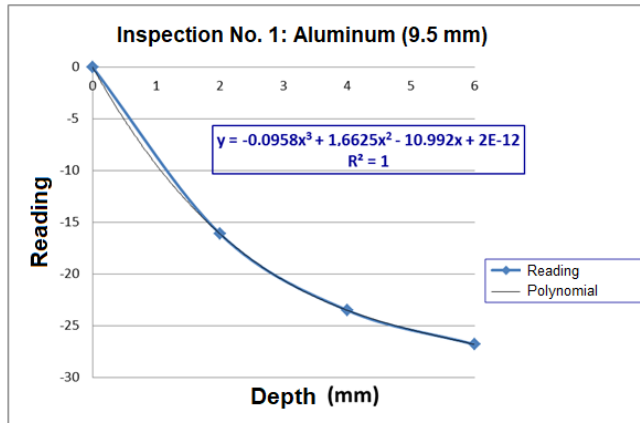


Fig. 9. Inspection No. 1 - 9.5 mm thick aluminum plate

b) *INSPECTION No. 2*

Aluminum plate with 7.6 mm thickness. Sensitivity control at maximum.

TABLE II. RESULTS OF INSPECTION No. 2.

Test	Crack Dimensions (mm)		Reading	
	Depth	Width	A	B
0	0.00	0.00	0.0	0.0
1	0.23	0.25	-0.7	-7.8
2	0.33	0.25	-1.6	-12.1
3	0.48	0.25	-2.7	-17.0
4	0.60	0.25	-3.8	-19.3

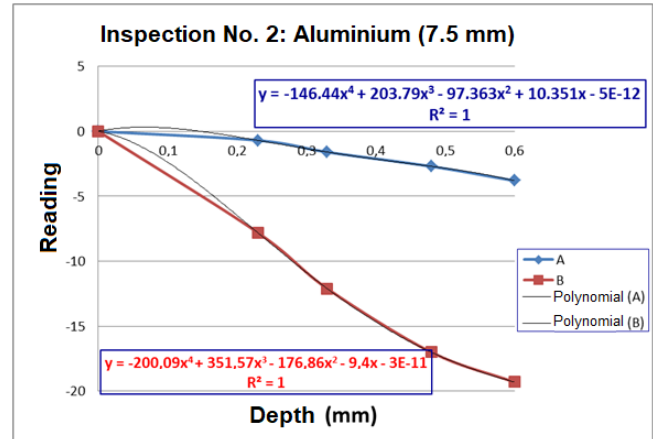


Fig. 10. Inspection No 2 - 7.6 mm thick aluminum plate.

c) *INSPECTION No. 3*

Aluminum plate with 3.0 mm thickness. Sensitivity control at maximum.

TABLE III. RESULTS OF INSPECTION No 3.

Test	Crack Dimensions (mm)		Reading	
	Depth	Width	A	B
0	0.00	0.00	0.0	0.0
1	0.23	0.19	-0.7	-4.2
2	0.26	0.19	-1.2	-6.4
3	0.34	0.19	-1.9	-12.2
4	0.41	0.19	-2.5	-15.2
5	0.56	0.19	-3.7	-17.8

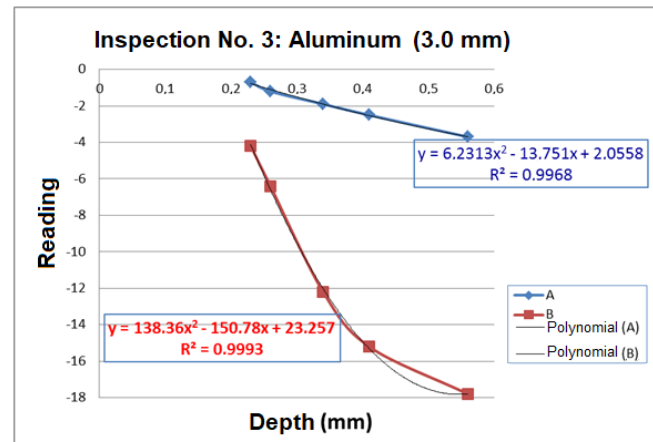


Fig. 11. Inspection No 3 - 3.0 mm thick aluminum plate.

d) *INSPECTION No. 4*

Non-magnetic steel plate 3.2 mm thick. Sensitivity control at maximum.

TABLE IV. RESULTS OF INSPECTION No. 4.

Test	Crack Dimensions (mm)		Reading	
	Depth	Width	A	B
0	0.00	0.00	0.0	0.0
1	0.20	0.19	-0.2	3.1
2	0.36	0.19	-0.8	9.4
3	0.58	0.19	-3.2	233

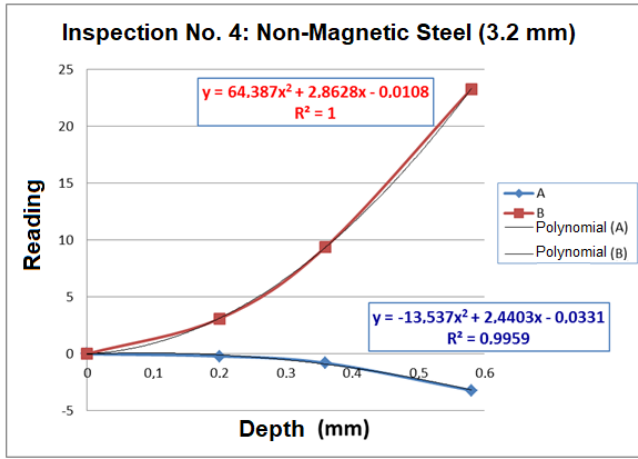


Fig. 12. Inspection No 4 – 3.2 mm thick non-magnetic steel plate.

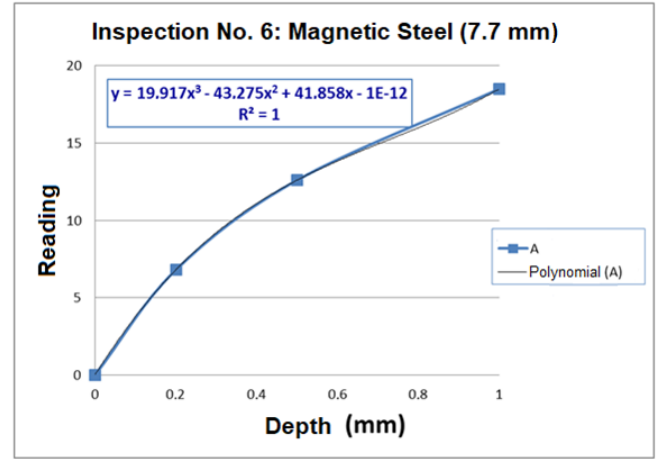


Fig. 14. Inspection No 6 - 7.7 mm thick magnetic steel plate.

e) *INSPECTION No. 5*

Magnetic steel plate 11.5 mm thick. Sensitivity control at minimum.

TABLE V. RESULTS OF INSPECTION No. 5.

Test	Crack Dimensions (mm)		Reading
	Depth	Width	
0	0.0	0.00	0.0
1	2.0	0.42	6.9
2	4.0	0.42	10.0
3	8.0	0.42	11.5

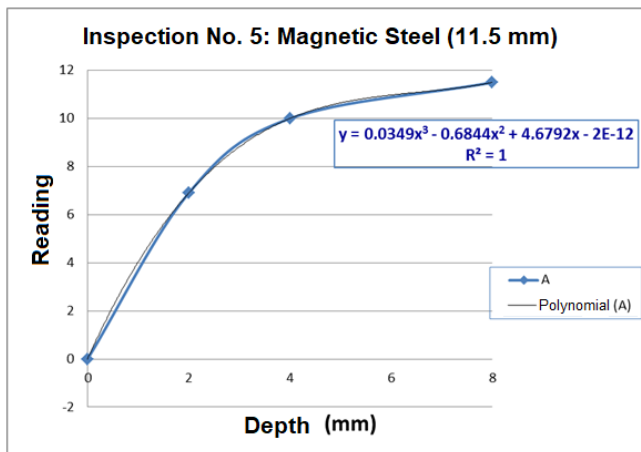


Fig. 13. Inspection No 5 – 11.5 mm thick magnetic steel plate.

f) *INSPECTION No. 6*

Magnetic steel plate 7.7 mm thick. Sensitivity control at maximum.

TABLE VI. RESULTS OF INSPECTION No. 6.

Test	Crack Dimensions (mm)		Reading
	Depth	Width	
0	0.0	0.00	0.0
1	0.2	0.23	6.8
2	0.5	0.23	12.6
3	1.0	0.23	18.5

g) *INSPECTION No. 7*

Inconel[®] plate 0.5 mm thick. Sensitivity control at maximum.

TABLE VII. RESULTS OF INSPECTION No. 7.

Test	Crack Dimensions (mm)		Reading	
	Depth	Width	A	B
0	0.00	0.00	0.0	0.0
1	0.10	0.17	-0.8	1.0
2	0.19	0.17	-2.4	3.5
3	0.20	0.17	-2.6	4.0

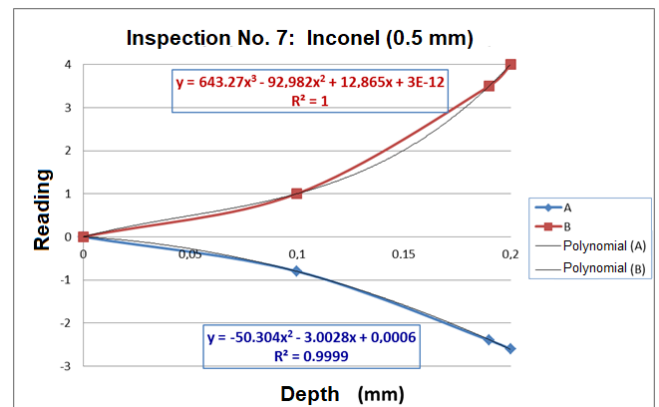


Fig.15. Inspection No 7 - 0.5 mm thick inconel™ plate.

C. *Measurement of Non-Conductive Layer Thickness on Conductive Base*

Figure 15 shows the graph of the instrument reading as a function of the probe's distance from an aluminum surface (conductive base). For other types of base material, the readings will be different. In the graph, it is noted that from a certain distance, in this case 7.0 mm, the reading remains constant, as the electromagnetic field of the coil no longer reaches the metallic base.

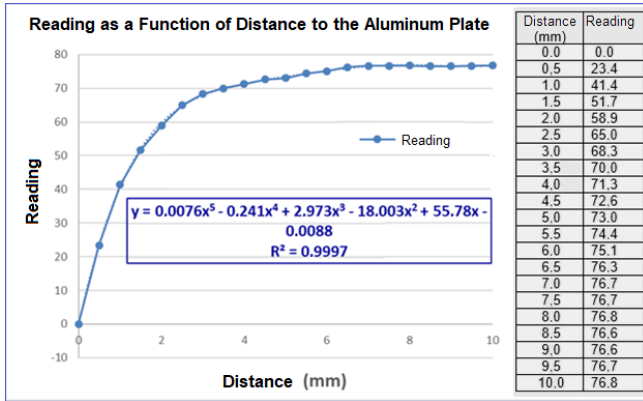


Fig. 16. Measurement of the thickness of non-conductive layer on aluminum plate.

1) Identification of metals and alloys

By fixing the frequency control in a certain position and bringing the probe close to the surface of some conductors, the meters will give different indications for each type of conductor. In non-ferromagnetic materials this change in reading is due to the different conductivities of each part. The readings on the meters can be converted to % IACS, this requires conductivity standards that cover a range of conductive materials. The conductivities of these standards must be well known. Measurements are then taken with the instrument to establish the relationship between the measurements in IACS and the readings obtained with the equipment.

By placing the probe in contact with ferromagnetic materials, the equipment reading is influenced by the conductivity of the material and, on a larger scale, by its permeability. That's why the meter reading is greatly increased and the immediate differentiation between non-magnetic and magnetic materials is immediate.

Table VIII shows the values obtained when the probe is placed in contact with some conductive materials. It is not known if the samples used are pure, if they have received some kind of treatment and their conductivities are not known either. The values presented here only serve to show the feasibility of the instrument in measuring the conductivity of non-ferromagnetic materials and differentiating them from ferromagnetic materials.

To obtain the values in Table VIII, the LIFT-OFF/FREQ control was set. at its maximum position, that is, frequency close to 55 kHz. The probe was placed in contact with a copper sample and the BALANCE control was varied until the reading indicated zero, which was the reference value. The other values were obtained by placing the probe in contact with different materials. From the table it can be seen that the measurements for ferromagnetics are always larger than those for non-ferromagnetics.

TABLE VIII. IDENTIFICATION OF METALS.

Material	Reading
Copper	0.0
Aluminum	-1.1
Bronze	-2.7
non-magnetic steel	1.4
Stainless steel	14.8
Cast iron	25.8

Using other positions of the LIFT-OFF/FREQ and BALANCE controls increases the measurement values and has greater sensitivity. This is recommended to distinguish one material from another which has similar conductivity values.

IV. CONCLUSIONS

For instruments of the type developed in this work, it can be said that in applications such as surface crack detection, material classification and assessment of non-conductive layer thickness on a conductive base, it is superior to equipment that does not use electromagnetic principles. This is because of the accuracy and ease of carrying out the inspection.

In the particular case of the device designed here, in addition to the advantages mentioned in the previous paragraph, the simplicity of the circuits, the low cost of the electronic components used and the possibility of finding them in the trade, facilitating possible maintenance

In general, the instrument is capable of performing all the proposed functions, namely:

- Detection of surface discontinuities in conductive material.
- Assessment of the depths of the detected discontinuities.
- Classification of materials according to conductivity variation.
- Thickness measurement of non-conductive layers on a conductive base.

Despite not having made measurements of the thickness of metal sheets, it can be said that the instrument also applies to this function (with a limitation of up to 6 mm).

The main features of the equipment are:

- High speed response to imperfections. The operator is never able to pass the probe over a crevice faster than the meter responds. On the other hand, the indication is maintained until the probe leaves the area of influence of the fault.
- Possibility of adjustment to compensate for the lift-off effect.
- Ease of operation and possibility of making coils and probes for special applications.
- Continuous frequency variation, allowing inspection of most metals.
- Possibility of using an alarm or data acquisition system to evaluate the results of tests carried out in series.
- Small, light in weight, when working with analog meter only, power consumption is low, enabling the use of rechargeable batteries.

Due to the complexity of finding an expression that gives the relationship between the signal in the meter and the dimensions of the fault, and also because it is outside the scope of this work, this analysis was not carried out. Generally speaking, meter readings increase with the depth of the cracks.

ACKNOWLEDGMENT

The authors would like to thank the following Brazilian institutions: Nuclear Technology Development Center (CDTN), Brazilian Nuclear Energy Commission (Cnen), Research Support Foundation of the State of Minas Gerais (Fapemig), Brazilian Council for Scientific and Technological Development (CNPq).

REFERENCES

- [1] R. Grimberg, "Electromagnetic Nondestructive Evaluation: Present and Future," *Strojniški vestnik - Journal of Mechanical Engineering*, vol. 57, no.3, pp. 204-217, 2011. DOI: 10.5545/sv-jme.2010.171.
- [2] Hui, S.K.; Jang, H.; Gum, C.K.; Song, C.Y.; Yong, H.K. A new design of inductive conductivity sensor for measuring electrolyte concentration in industrial field. *Sensors and Actuators A: Physical*. 2020. DOI: 10.1016/j.sna.2019.111761.
- [3] M. Lu, W. Zhu, L. Yin, A. J. Peyton, W. Yin, Z. Qu, "Reducing the Lift-Off Effect on Permeability Measurement for Magnetic Plates From Multifrequency Induction Data," *IEEE Transactions on Instrumentation and Measurement*, vol. 67, no. 1, pp. 167-174, January 2018. DOI: 10.1109/TIM.2017.2728338.
- [4] J. Harms and T.A. Kern, "Theory and Modeling of Eddy Current Type Inductive Conductivity Sensors," *Engineering Proceedings*, vol. 6, no. 37, pp 1 – 6. 2021. DOI: 10.3390/I3S2021Dresden-10103.
- [5] Y. Yating and D. Pingan, "Two approaches to coil impedance calculation of eddy current sensor," *Proc. IMechE*, vol. 222 Part C, pp. 507 – 515. *Journal of Mechanical Engineering Science*. DOI: 10.1243/09544062JMES395.
- [6] C. Chong and F. Zhang, *Electromagnetic Testing - Eddy Current Mathematics*. My ASNT Level III Pre-Exam Preparatory Self Study Notes. 2014.
- [7] ASM - American Society for Metals, *Nondestructive Testing*. Metals Park, Ohio: ASM International. 1995.
- [8] General Dynamics - Convair Division, *Nondestructive Testing Eddy Current, Classroom Training Handbook*. 2nd Edition. San Diego. 1979.
- [9] J. Millman and C.C. Halkias, *Integrated Eletronics Analog and Digital Circuits and Systems*. 50 Edition. Tata McGraw - Hill Education, New Delhi, 1991.
- [10] H.L. Fernandez-Canque, *Analog Electronics Applications*. 1st Edition. Imprint CRC Press. Boca Raton. 2016. DOI: 10.1201/9781315371252.
- [11] G.A. Leclerq, *Transistores y Semiconductores Industriales..* Marcombo-Boixareu Editores. Barcelona, 1978.
- [12] A.P. Godse and U.A. Bakshi, *Analog Electronic Circuits*. Technical Publications; 1st edition. Pune, India. 2019.
- [13] A. Soares, "Aplicações das Correntes de Foucault na Detecção de Descontinuidades em Tubos da Zircaloy," Master's degree dissertation, Escola de Engenharia da Universidade Federal de Minas Gerais (UFMG). Belo Horizonte, MG, Brazil. 1976.
- [14] *Motorola Inc.*, Motorola Small-Signal Transistors, FETs and Diodes Device Data. D11 261D, Rev. B. Phoenix. 1997.
- [15] *Texas Instruments Inc.*, Transistor Circuit Design. New York. MacGraw-Hill Book. 1965.
- [16] A.Z. Mesquita, *Digital Instrument for Eddy Current Tests*. 1. ed. Riga Latvia: Novas Edições Acadêmicas. SIA OmniScriptum Publishing, v. 1. 116p. 2018. (in Portuguese).